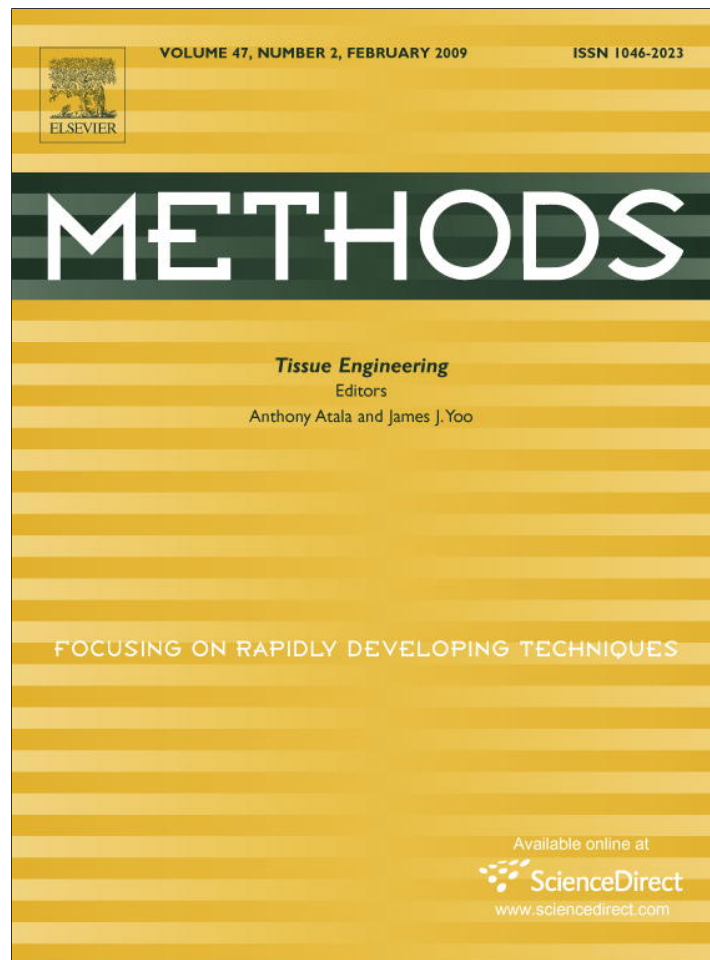


Provided for non-commercial research and education use.
Not for reproduction, distribution or commercial use.



This article appeared in a journal published by Elsevier. The attached copy is furnished to the author for internal non-commercial research and education use, including for instruction at the authors institution and sharing with colleagues.

Other uses, including reproduction and distribution, or selling or licensing copies, or posting to personal, institutional or third party websites are prohibited.

In most cases authors are permitted to post their version of the article (e.g. in Word or Tex form) to their personal website or institutional repository. Authors requiring further information regarding Elsevier's archiving and manuscript policies are encouraged to visit:

<http://www.elsevier.com/copyright>



Contents lists available at ScienceDirect

Methods

journal homepage: www.elsevier.com/locate/ymeth

Composite scaffolds for the engineering of hollow organs and tissues

Daniel Eberli, Luiz Freitas Filho, Anthony Atala, James J. Yoo *

Wake Forest Institute for Regenerative Medicine, Medical Center Boulevard, Winston Salem, NC 27154-1094, USA

ARTICLE INFO

Article history:

Accepted 16 October 2008

Available online 24 October 2008

Keywords:

Composite scaffolds

PGA

Acellular bladder matrix

Hollow organs

Bladder

ABSTRACT

Several types of synthetic and naturally derived biomaterials have been used for augmenting hollow organs and tissues. However, each has desirable traits which were exclusive of the other. We fabricated a composite scaffold and tested its potential for the engineering of hollow organs in a bladder tissue model. The composite scaffolds were configured to accommodate a large number of cells on one side and were designed to serve as a barrier on the opposite side. The scaffolds were fabricated by bonding a collagen matrix to PGA polymers with threaded collagen fiber stitches. Urothelial and bladder smooth muscle cells were seeded on the composite scaffolds, and implanted in mice for up to 4 weeks and analyzed. Both cell types readily attached and proliferated on the scaffolds and formed bladder tissue-like structures *in vivo*. These structures consisted of a luminal urothelial layer, a collagen rich compartment and a peripheral smooth muscle layer. Biomechanical studies demonstrated that the tissues were readily elastic while maintaining their pre-configured structures. This study demonstrates that a composite scaffold can be fabricated with two completely different polymer systems for the engineering of hollow organs. The composite scaffolds are biocompatible, possess adequate physical and structural characteristics for bladder tissue engineering, and are able to form tissues *in vivo*. This scaffold system may be useful in patients requiring hollow organ replacement.

© 2008 Elsevier Inc. All rights reserved.

1. Introduction

Biomaterials for tissue engineering provide a three-dimensional environment that allows cells to develop new tissues with appropriate structure and function [1]. These materials are usually designed to replicate the biologic and physical function of the native extra cellular matrix (ECM) found in the body to enhance tissue formation. Thus, an ideal biomaterial should be biocompatible and support tissue growth without inducing severe inflammatory processes [2] that lead to foreign-body giant cell formation or fibrous scarring. In addition, the biomaterial should provide adequate structural support to the neo-organ during tissue development and degrade gradually over time as cells undergo spatial organization. This is especially important for the engineering of hollow organs such as blood vessels, esophagus and bladders, where biomaterials serve as a separator that interfaces with the content of the cavity and the viscera. Therefore, biomaterials which constitute a scaffolding system for these organs should serve as a barrier while accommodating sufficient amounts of cells that facilitate tissue development.

Traditionally, two main classes of biomaterials have been utilized for the engineering of hollow organs; acellular matrices derived from donor tissues [3–8], (e.g., bladder submucosa (lamina propria) and small intestinal submucosa), and synthetic poly-

mers such as polyglycolic acid (PGA) [9,10], polylactic acid (PLA), and poly(lactic-co-glycolic acid) (PLGA). These materials have been tested in respect to their biocompatibility in the host tissues [11,12]. Each type of biomaterials has desirable traits which are exclusive of the other. Acellular tissue matrices possess the desired biocompatibility [11–13], contain biomimetic factors [14–16] that promote tissue development and have adhesion domain sequences (e.g., RGD) that may assist in retaining the phenotype and activity of many types of cells [17]. These matrices are known to slowly degrade upon implantation and are usually replaced and remodeled by ECM proteins synthesized and secreted by transplanted or ingrowing cells [18–25]. In contrast, synthetic polymers can be manufactured reproducibly on a large scale with controlled properties of their strength, degradation rate and ultrastructure [26,27]. Both classes of biomaterials have been used either with or without cells for the tissue engineering of hollow organs and tissues, including the bladder [5,6,10], urethra [3,4,9], ureter [7], esophagus [8,28], intestine [28], uterus [29], vagina [29,30] and blood vessels [31,32].

Most hollow organs are organized in a similar fashion, consisting of epithelium or endothelium on the lumen surrounded by a collagen rich connective tissue and muscle layer. Epithelial or endothelial layer serves as a barrier that prevents the content of the lumen from permeating into the body cavity. The collagen rich layer and muscle tissue surrounding the epithelium/endothelium maintain the structural integrity of the organ. The cells composing these layers interact with each other and other proteins to regulate cellular differentiation and function [14,33]. Thus, an ideal

* Corresponding author. Fax: +1 336 713 7290.

E-mail addresses: daniel.eberli@usz.ch (D. Eberli), lffreitasf@terra.com.br (L.F. Filho), aatala@wfubmc.edu (A. Atala), jyoo@wfubmc.edu (J.J. Yoo).

biomaterial must provide an environment in which corresponding cell types could interact with each other to guide appropriate regulation that governs adhesion, proliferation, migration, and differentiation can occur. Therefore, multiple cell types are required to create a hollow organ with the appropriate “layered” structure. Since each of these cell types favors different conditions for optimal growth and differentiation, ideal tissue engineering strategies must take these factors into account.

Biomaterials for hollow organs should provide structural support for distinct cell layers, including an adequate surface for stable attachment of epithelial/endothelial cells. It should also provide adequate biomechanical support to harbor a high density of smooth muscle cells on the exterior surface without collapsing prematurely. The development of specialized biomaterials consisting of these components might improve current tissue engineering techniques. Herein, we designed and fabricated a novel composite scaffold that utilizes both the acellular tissue matrix and synthetic polymers. This scaffold system was created by bonding the two heterogeneous materials together with threaded collagen fiber stitches to form a dual layered structure. Specifically, the acellular tissue matrix serves as a barrier that would prevent the luminal content from permeating to the viscera while providing optimal surface for epithelial cell adherence. The synthetic polymer layer with large pores is designed to accommodate sufficient numbers of muscle cells and maintain structural integrity of the scaffold at the same time. In this study, we examined the validity of composite scaffolds using a bladder tissue model for their possible utility in engineering of other hollow organs.

2. Description of methods

2.1. Preparation of composite biomaterial

Composite scaffold was created by using 2 different materials: acellular bladder matrix (ABM) and polyglycolic acid (PGA, US Surgical Corp. Norwalk, CT, USA). Both materials have been shown to be biocompatible and safely used clinically [11,12,34,35]. Acellular tissue matrix, obtained from porcine bladders, was processed using a multiple-step detergent wash protocol developed in our laboratory [12,16]. Each porcine bladder was rinsed with running tap water, and placed in a -20°C freezer overnight. The bladder was thawed in cool water, opened with sharp scissors, and placed flat on a table. The muscle layer was micro-dissected and removed with sharp scissors while the epithelial cell layer was removed by mechanically scraping the epithelium with a No. 10 surgical blade. The remaining tissue, consisting mainly of lamina propria, was placed in a container filled with 0.9% normal saline followed by continued agitation on an elliptical shaker at 4°C . The acellular matrix was treated with distilled water for 2 days to lyse the cells residing within the tissue. Distilled water was changed twice each day. Subsequently, the tissues were treated with 1% Triton X100 and 0.1% ammonium hydroxide in a stirring flask at 4°C for 7 days. The detergent was exchanged daily. Subsequently, the bladder matrix was rinsed with distilled water at 4°C for 2 days followed by a treatment with phosphate buffered saline (PBS) for 24 h. Small matrix samples were cut and analyzed by hematoxylin and eosin. A second round of detergent wash procedure was used if the matrices were not entirely free of cellular content. The bladder matrix was trimmed to the desired size and stored frozen at -80°C until needed.

To bond the ABM to the PGA, we initially used a heat bonding technique at 200°C for 80 min, followed by lyophilization and sterilization. However, the heat and lyophilization denatured the collagen which may have influenced the biologically active molecules associated with the matrix [16]. Therefore, we decided to keep the biomaterial in liquid [36] during the process and use a physical stitching method instead.

The ABM was placed on a pre-configured PGA non-woven felt (60 mg/cc, 123 denier 56 filament, US Surgical Corp. Norwalk, CT, USA) and stretched uniformly until the dimension remained reasonably constant. A light scrim of PGA was placed on the lumen side (top) of the collagen. This scrim was composed of a one layer PGA mesh and is used to prevent the locking fiber from cutting through the ABM. This ensures that both materials are stably stitched together. The entire structure was held together by the frictional grip of these fibers locking the collagen matrix into the system. The composite structure was then fed into a Hunter 11'' Needle loom tacker (Hunter Inc., Reston, VA). The loom tacker passed barbed needles through the composite structure, pulling individual filaments through in the “Z” direction. The composite was then turned over and passed through the needle loom a second time to strengthen the bonding. During manufacturing of the composite scaffold, care was taken to maintain the correct orientation of the ABM layer. The final composite biomaterial consisted of a two layered structure with a thick PGA layer on one side and an ABM layer on the other. This biomaterial has excellent surgical handling qualities, is highly flexible and can be sutured easily.

SEM and biomechanical testing was performed on every batch of the materials prior to in vivo use and these tests showed stable bonding with a high reproducibility. The material was stored at -20°C until use.

2.2. Cell cultivation and seeding

We used primary cells harvested from canine bladders using established protocols [10,37–39]. Bladder tissue was microdissected, and the mucosal and muscular layers were separated. Approximately, 1×1 cm sized mucosal tissue with the urothelial side facing up into a 10 cm culture dish. The mucosal surface was gently scraped with a No. 10 scalpel under sterile conditions. The detached cell clusters were confirmed using phase microscopy and placed in serum-free keratinocyte growth medium (Keratinocyte SFM, Gibco, Grand Island, NY) containing 5 ng/mL epidermal growth factor and 50 cLg/mL bovine pituitary extract.

The muscle layer was cut in small tissue fragments of 1×1 mm and placed onto a dry 10 cm culture dish. After 10 min, Dulbecco's Modified Eagle's Medium (DMEM; Gibco, Grand Island, NY) supplemented with 10% fetal calf serum was carefully added. The cells were incubated at 37°C in a humidified atmosphere containing 5% CO_2 . Both urothelial and smooth muscle cells were expanded separately until desired cell numbers were obtained. In these experiments, cells less than passage 5 were used for seeding.

The biomaterial was cut into 1×1 cm pieces and placed in 70% alcohol for 6 h in order to minimize potential bacterial contaminants. No permanent sterilization was used in this study. The expanded urothelial and smooth muscle cells were trypsinized, washed, and collected as a pellet. Urothelial cells were seeded onto the ABM surface of the composite biomaterial at a concentration of 1×10^7 cells per cm^2 and the construct was then incubated in serum-free keratinocyte growth medium for 2 days. Subsequently, the biomaterial was turned over and smooth muscle cells were seeded onto the PGA side of the construct at a concentration of 2×10^7 cells per cm^2 . The seeded constructs were then placed in DMEM supplemented with 10% fetal calf serum for an additional 2 days before implantation. Controls consisting of PGA only or ABM only were seeded following the same protocol.

2.3. Scanning electron microscopy (SEM)

For ultrastructural analysis, composite biomaterials were fixed in a 2.5% glutaraldehyde solution containing 0.085 M cacodylate buffer for 1 h. All samples were dehydrated through a graded series of ethanol and were eventually stored at 4°C . After critical point

drying, samples of material were sputter-coated with (Hommur V) gold and platinum and analyzed using a scanning electron microscope (SEM, Leo 1450 VP) at various magnifications.

SEM confirmed the bonding of the two biomaterials (Fig. 1). A thick collagen layer was formed by the ABM. The penetrating fibers used to bond the two biomaterials together were clearly visible on the SEM images. The non-woven PGA on the opposite side was porous.

2.4. Biomechanical testing

Rectangular tissue strips measuring 30×10 mm were used for biomechanical testing. The biomaterials were placed in PBS for 4 h prior to testing. Tensile tests (Instron model 5544, MA, USA) were performed by elongating the tissue strips longitudinally at a speed of 0.05 mm/s with a preload of 0.2 N until failure. The grip-to-grip spacing was approximately 20 mm. All specimens were tested at room temperature and kept moist. The maximum tensile strength (N/cm) and strain forces (MPa), were determined and analyzed. Further, the Young's modulus was calculated to evaluate the stiffness and elasticity of the biomaterial. Native bladder wall served as a normal control.

The results showed that the composite biomaterial has favorable biomechanical characteristics that are comparable to those of native bladder tissue (Fig. 2). Five samples were measured in each group. The tensile strain at failure was 1.1 ± 0.1 mm/mm for the composite and 1.3 ± 0.2 mm/mm for native bladder. This difference was not significant. The tensile stress at break was 1.5 ± 0.4 MPa for the composite biomaterial and 0.77 ± 0.2 MPa for native bladder ($p=0.006$). The load at break was 35.8 ± 7.1 N for the composite biomaterial and 18.5 ± 3.2 N for native bladder ($p=0.003$). The calculated Young's modulus was 0.0020 ± 0.0005 for the composite biomaterial and 0.0011 ± 0.0003 for native bladder ($p=0.008$). The statistical differences in the biomechanical tests do not reflect true biological differences, but rather indicate narrow standard deviations due to successful standardization of this delicate process. Since bioabsorbable materials were used in this study a slightly stronger composite is desirable. The degradation of the biomaterials will weaken the material over time until the host begins to support the construct by newly synthesized collagen fibers.

2.5. Porosity assessment

Most hollow organs require a water tight repair. In esophageal, gastric, intestinal and bladder engineering, leakage from the biomaterial leads to early inflammation and infection which may result in the death of the patient. Therefore, the porosity of the biomaterials was assessed before seeding with cells, after cell seeding, and after 14 and 28 days in vivo. We used the flow through

method [40] which defines porosity as the flow of water through the biomaterial per unit time and per unit surface area at a defined pressure.

For this test the biomaterial was clamped between two flat metal plates with central holes of 0.5 cm^2 surface area. Flexible tubing was connected to one side of the metal plate applying static water pressure. The static pressure head was defined by the difference in height between the water level and the specimen. Biomaterials were placed in the apparatus and subjected to the static pressure for 1 min and leakage flow was collected in a graduated cylinder for quantification of volume. The flow through porosity was defined as the amount of water flowing through one square centimeter of construct, measured in milliliters per minute, at a pressure of 120 mmHg. All specimens were tested at room temperature and kept moist.

The unseeded composite biomaterial had a porosity of 506.2 ± 7.1 ml/min/cm² while the PGA-only control had a porosity of 714.8 ± 7.7 ml/min/cm². After cell seeding, the porosity declined to 481.6 ± 28.4 ml/min/cm² for the composite biomaterial and to 634.5 ± 18.8 ml/min/cm² for the PGA-only control. The differences between all groups were significant ($p > 0.05$). The ABM-only control and all samples retrieved from in vivo experiments at 2 and 4 weeks were 100% water tight. The process of sewing the constructs together resulted in numerous needle induced holes into the ABM layer, thus increasing the porosity and flow. This indicates that in vivo cell proliferation and tissue formation is needed to achieve the ultimate goal of water tightness. Although the porosity index presented is a widely used method of comparing different biomaterials, it may not predict whether or not the composite biomaterial will leak in vivo.

2.6. In vivo evaluation

All procedures were performed in accordance with the institution's Animal Care and Use Committee. Twenty-four athymic mice (nu/nu, Charles River Laboratories Inc. Wilmington, MA, USA) were randomly assigned to 3 groups. Group 1 received the seeded composite biomaterial ($n=16$), while Group 2 and 3 served as controls and received seeded PGA constructs ($n=16$) and seeded ABM constructs ($n=16$), respectively.

All surgeries were performed under general anaesthesia (2% isoflurane). The area of surgery was disinfected with iodine solution. A 3 cm long incision was made on the dorsum of each mouse. In all groups, two seeded constructs were placed subcutaneously between the muscle and skin. The surgical wound was closed using absorbable running sutures. All animals survived the surgical procedure without noticeable complications. During the first 24 h, the mice received routine analgesia with buprenorphine (0.1 mg/kg) 2 times per day. Animals were housed together, allowed free access

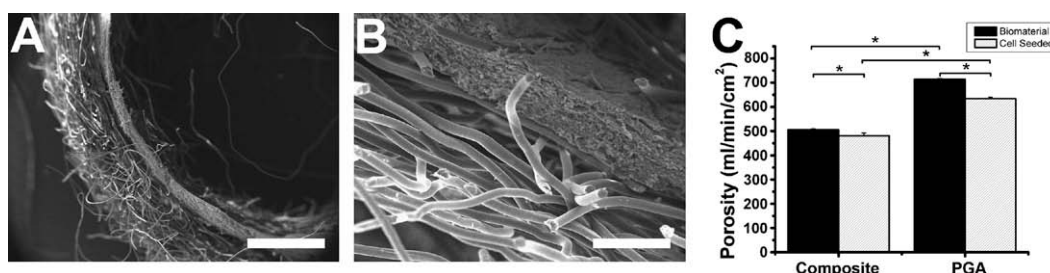


Fig. 1. Ultra structural analysis. (A and B) Scanning electron microscopy. The composite scaffolds, consisting of a naturally-derived collagen-based acellular matrix and polyglycolic acid polymers, are bonded after fabrication, and maintained their ultrastructural properties. Scale bar represents 2 mm (A) and 500 μm (B). (C) Porosity assessment by the flow-through method. The unseeded composite biomaterial shows a porosity of 506.2 ± 7.1 ml/min/cm² while the PGA-only control demonstrates a porosity of 714.8 ± 7.7 ml/min/cm². The relatively high flow-through porosity of the composite biomaterial is likely due to the bonding technique used, which punches hundreds of tiny holes into the ABM for suturing. After cell seeding, the porosity is reduced to 481.6 ± 28.4 ml/min/cm² for the composite biomaterial and to 634.5 ± 18.8 ml/min/cm² for the PGA-only control. All retrieved constructs at 2 and 4 weeks were water tight. The differences between all groups were significant ($p > 0.05$).

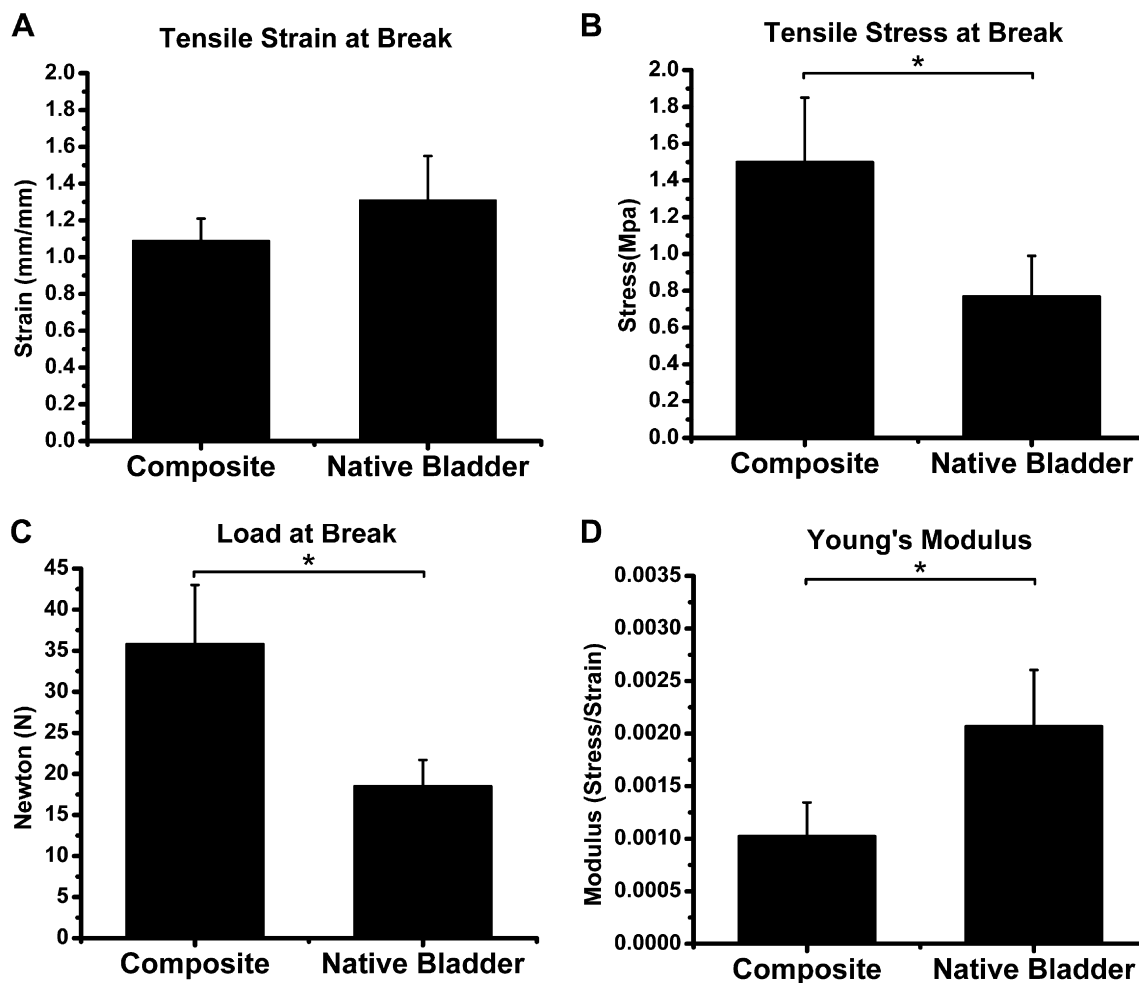


Fig. 2. Biomechanical analysis. The mechanical analysis shows that composite biomaterial has favorable biomechanical characteristics which are comparable to native bladder. (A) The tensile strain at break was 1.1 ± 0.1 mm/mm for the composite and 1.3 ± 0.2 mm/mm for native bladder (not significant). (B) The tensile stress at break was 1.5 ± 0.4 MPa for the composite biomaterial and 0.77 ± 0.2 Mpa for native bladder ($p=0.006$). (C) The load at break was 35.8 ± 7.1 N for the composite biomaterial and 18.5 ± 3.2 N for native bladder ($p=0.003$). (D) The calculated Young's modulus was 0.0020 ± 0.0005 for the composite biomaterial and 0.0011 ± 0.0003 for native bladder ($p=0.008$).

to food and water, and were maintained on a light-dark cycle of 12 h each.

Four animals from each group were sacrificed on day 14 and day 28 after implantation. At the time of sacrifice, the animals were euthanized by CO₂ followed by cervical dislocation. Immediately after euthanasia, the implant site was inspected and the engineered tissue retrieved. The retrieved constructs and the surrounding tissues were inspected grossly and histologically. Macroscopically, there was no evidence of infection or fibrosis, and the biomaterial was integrated into surrounding connective tissue. All samples showed signs of neo-vascularization (Fig. 3). Seeded ABM-only grafts were not able to form voluminous tissue and remained as a thin layer. PGA and the composite biomaterial both showed the formation of voluminous tissue (Fig. 3). The formation of voluminous tissue is indicative of cell proliferation within the constructs. This is only possible if the cells are provided with sufficient nutrients and oxygen. At 2 weeks, the volume of tissue resulting from seeded ABM, composite biomaterial and PGA were 36.1 ± 4.4 mm³, 99.7 ± 18.0 mm³ and 124.6 ± 8.5 mm³ ($p < 0.014$), respectively. All seeded constructs showed some reduction in volume at 4 weeks with 22.9 ± 7.6 mm³, 79.1 ± 11.0 mm³ and 104.3 ± 16.0 mm³ for seeded ABM, composite biomaterial and PGA ($p < 0.003$), respectively. Our results indicate a slight reduction in volume of the composite and the controls at 4 weeks. This might be due to the degradation of the PGA fiber loops, which starts at the interface to host tissue, making the retrieved sample appear smaller.

2.7. Histological analysis

For histological analysis, engineered bladder tissues were washed in PBS and embedded in tissue freezing medium (OCT compound; Miles, Elkhart, NJ). Cryosections of 6 μm thickness (Leica RM 2145) were analyzed with hematoxylin and eosin, Masson's trichrome and immunocytochemistry using cell specific antibodies. Urothelial cells were identified by probing tissue sections with polyclonal anti-pancytokeratins AE1/AE3 (Dako, Carpinteria, CA, Cat# M3515, Lot# 005500, 1:50), while smooth muscles were identified using anti-alpha-actin (Santa Cruz, Santa Cruz, CA, Cat# sc-32251, Lot# E0806, 1:20). As secondary antibodies, we used biotinylated horse anti-mouse antibody (Vector Laboratories, Burlingame, CA, Cat# BA 2000, Lot# R0719, 1:300). Detection was performed with the VectaStain ABC avidin-biotin detection kit (Vector Laboratories, Burlingame, CA) and visualized with the DAB chromogen. Tissue sections that were not incubated with primary antibody were used as negative controls.

Hematoxylin and Eosin staining of all samples showed high cellularity and good tissue organization, suggesting that new tissue was formed in vivo (Fig. 4). All materials showed excellent biocompatibility. There was a minimal mixed cellular infiltration that was devoid of lymphoid follicles or calcifications in all cases. The seeded ABM-only control samples showed both cell types attached to the thin biomaterial. However, a thick muscular compartment was absent.

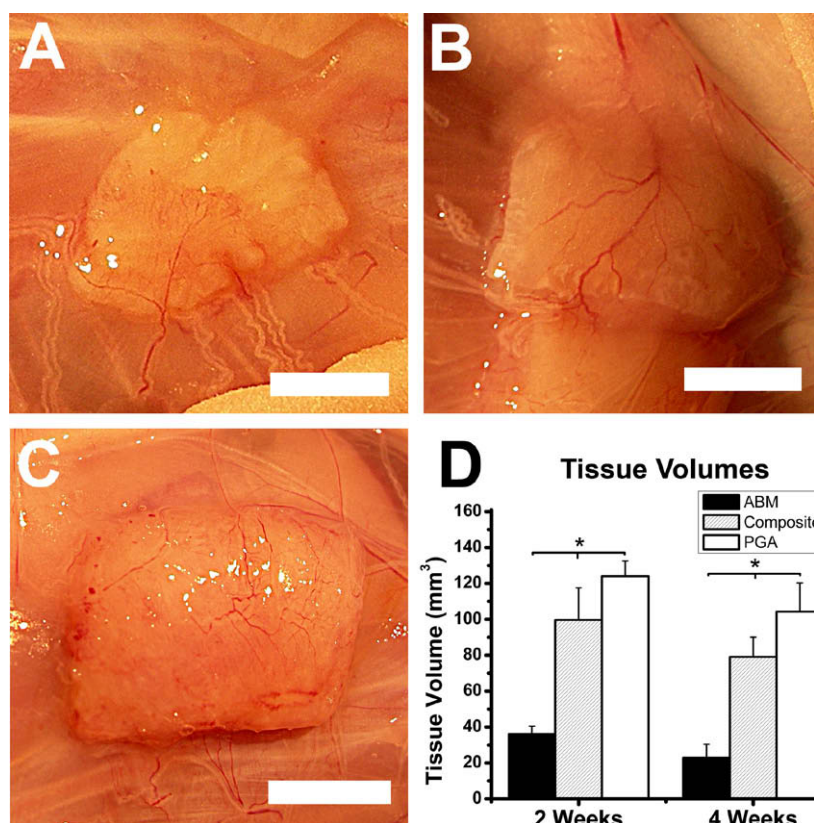


Fig. 3. Gross evaluation (A–C). Cell seeded scaffolds at retrieval. Seeded ABM-only (A) grafts were not able to form bulky tissue and remained as a thin layer. Composite biomaterial (B) and PGA (C) both showed the formation of bulky tissue (D) Volume assessment at 2 and 4 weeks. At 2 weeks the volumes for seeded ABM, composite biomaterial and PGA were 36.1 ± 4.4 , 99.7 ± 18.0 and 124.6 ± 8.5 mm³. The groups were all significantly different ($p < 0.014$). All seeded constructs showed some reduction in volume at 4 weeks with 22.9 ± 7.6 , 79.1 ± 11.0 and 104.3 ± 16.0 mm³ for seeded ABM, composite biomaterial and PGA. The groups were all significantly different ($p < 0.003$). Error bars represent Standard Error of the Mean (SEM).

Seeded PGA-only control constructs showed both cell types and a developed smooth muscle layer, but the interface between urothelial cells and smooth muscle cells was less distinct, with urothelial cells penetrating deep into the muscle layer. Only the composite biomaterial was able to maintain the specific organization of normal bladder tissue. The histological analysis revealed a distinct 3 layer architecture with a urothelial layer followed by a dense collagen layer followed by a thick muscle compartment (Fig. 4A). The urothelial layer was several cell layers thick, with smaller cells close to the basement membrane and larger cells 4–5 cell layers away. In addition, the seeded smooth muscle cells had begun to align and form compact muscle bundles. Immunohistochemistry confirmed the phenotype of the urothelial and smooth muscle cells.

2.8. Western blot analysis

Western blot analysis for anti-pancytokeratins AE1/AE3, anti-desmin (BD Biosciences, San Jose, CA, 1:50) and anti-alpha-actin was performed on protein isolated from retrieved tissue specimens ($n=4$). To minimize contamination from host myo-fibroblasts we have used only the center sections of the retrieved constructs for analysis. Implanted composite constructs without cells were prepared in the same manner and these extracts were used as controls for the Western blotting assays. Protein samples were prepared using routine extraction methods. The specimens were rapidly homogenized in standard lysis buffer (Tris-20 1 M, NaCl 3 M, Triton 10% with protease inhibitor) and incubated in the buffer on ice. After 30 min on ice, the lysates were centrifuged at 12,500g for 15 min and the supernatants were kept. The protein concentration in each supernatant was determined using the Bio-Rad DC Protein

Assay Kit (Bio-Rad, Hercules, CA). Aliquots of 20 µg total protein were then separated via SDS-PAGE (12% gel; 120V and 200 mA). The proteins were transferred to nitrocellulose membranes. After transfer, the membranes were blocked with 5% bovine serum albumin (BSA). The blots were probed with the primary antibodies overnight at 4 °C, washed, and subsequently treated with secondary antibody conjugates for 1 h at room temperature. Immunoblots were treated with an enzyme-linked chemiluminescence reagent (Western Lightning Plus, Perkin Elmer, Boston, MA) and exposed to X-ray film for 30 s to 5 min. Samples retrieved at 4 weeks after implantation showed the presence of pancytokeratin AE1/AE3, actin and desmin, indicating that urothelial and smooth muscle cells had developed in the implants. Control composite biomaterial implanted in vivo for 4 weeks without prior cell seeding remained negative for these markers.

2.9. Statistical analysis

In this report all data were expressed as averages and standard deviations, and these were analyzed using unpaired *t*-tests (porosity test and mechanical studies) with statistical software (SPSS V11; SPSS Inc., Chicago, IL). A *p*-value of less than 0.05 was considered significant. The tissue volumes were analyzed by one-way ANOVA. If significant, the groups were further analyzed by Bonferroni post-hoc testing. An alpha of $p > 0.05$ was considered significant.

3. Concluding remarks

Scaffold designing for hollow organs requires a special consideration as the biomaterials constituting a scaffolding system should

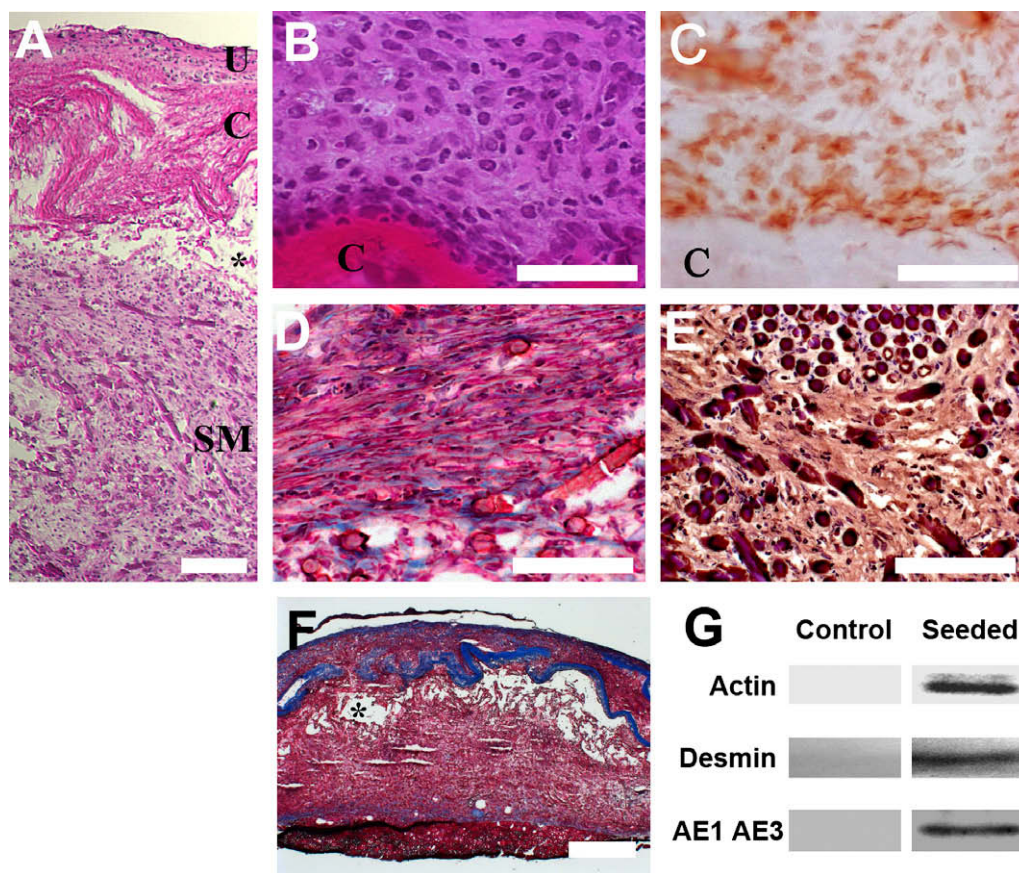


Fig. 4. Histology and western blot analysis. (A) Histology of cell seeded composite scaffolds 4 weeks after implantation showed characteristics of native bladder tissue: urothelial (U) and smooth muscle cell (SM) layers. The collagen layer (C) formed a structure similar to the basement membrane and the lamina propria. Due to the differences in stiffness of the 2 materials used the sectioning was technically demanding. The asterisk indicates a rupture of the composite biomaterial due to shear forces during sectioning. Hematoxylin and Eosin stain, 50 \times , Scale bar represents 100 μ m. (B) Urothelial cells seeded onto the collagen (C) surface of the composite biomaterial for a mature urothelial layer. Hematoxylin and Eosin stain 200 \times , Scale bar represents 50 μ m. (C) Immunohistochemistry confirming the urothelial phenotype (anti-pancytceratine AE1/AE3), 200 \times , Scale bar represents 50 μ m. (D) The seeded smooth muscle cells started to organize in an aligned fashion and form compact muscle bundles within the PGA part of the composite biomaterial. Hematoxylin and Eosin stain 200 \times , Scale bar represents 50 μ m. (E) Immunohistochemistry was able to confirm the smooth muscle phenotype (anti-actin). 200 \times , Scale bar represents 50 μ m. (F) The trichrome stain again revealed the distinct 3 layer architecture with a urothelial layer followed by a dense collagen layer (blue) followed by a thick muscle compartment. The asterisk indicates a rupture of the composite biomaterial due to shear forces during sectioning. 20 \times , Scale bar represents 500 μ m. (G) Western blot analyses using anti-alpha-actin, anti-desmin and anti-pancytokeratins AE1/AE3 demonstrate the presence of protein expression characteristic for urothelial cells and smooth muscle cells within the cell seeded matrices.

serve as a barrier between the cavity and the viscera while accommodating sufficient amounts of cells that facilitate tissue development. In this article we configured a composite scaffolding system by bonding a collagen matrix to PGA polymers with threaded collagen fiber stitches. This scaffolding system accommodates a large number of cells on one side and serves as a barrier on the other side. We show that the composite scaffolds made from ABM and PGA remain biocompatible, possess ideal physical and structural characteristics for hollow organ applications, and are able to form tissues *in vivo*. This scaffold system may be useful in the future in patients requiring hollow organ and tissue replacement.

Acknowledgments

We thank Mr. John Gray (Biomedical Structures LLC, Warwick, RI) for bonding of the composite scaffolds and Dr. Jennifer L. Olson for editorial assistance. This research was supported, in part, by the Gebert Ruef Stiftung, Switzerland, Astra Zeneca, Switzerland and the Swiss Urological Association.

References

[1] A. Atala, *Clin. Plast. Surg.* 30 (2003) 649–667.

- [2] A. Atala, *Pediatr. Res.* 63 (2008) 569–575.
 [3] B.P. Kropp, J.K. Ludlow, D. Spicer, M.K. Rippey, S.F. Badylak, M.C. Adams, M.A. Keating, R.C. Rink, R. Birhle, K.B. Thor, *Urology* 52 (1998) 138–142.
 [4] F. Chen, J.J. Yoo, A. Atala, *Urology* 54 (1999) 407–410.
 [5] J.J. Yoo, J. Meng, F. Oberpenning, A. Atala, *Urology* 51 (1998) 221–225.
 [6] B.P. Kropp, M.K. Rippey, S.F. Badylak, M.C. Adams, M.A. Keating, R.C. Rink, K.B. Thor, *J. Urol.* 155 (1996) 2098–2104.
 [7] A. Shokeir, Y. Osman, M. El-Sherbiny, M. Gabr, T. Mohsen, M. El-Baz, *Eur. Urol.* 44 (2003) 603–609.
 [8] Y. Urita, H. Komuro, G. Chen, M. Shinya, S. Kaneko, M. Kaneko, T. Ushida, *Pediatr. Surg. Int.* 23 (2007) 21–26.
 [9] L. Olsen, S. Bowald, C. Busch, J. Carlsten, I. Eriksson, *Scand. J. Urol. Nephrol.* 26 (1992) 323–326.
 [10] F. Oberpenning, J. Meng, J.J. Yoo, A. Atala, *Nat. Biotechnol.* 17 (1999) 149–155.
 [11] J.L. Pariente, B.S. Kim, A. Atala, *J. Biomed. Mater. Res.* 55 (2001) 33–39.
 [12] J.L. Pariente, B.S. Kim, A. Atala, *J. Urol.* 167 (2002) 1867–1871.
 [13] D. Eberli, R. Susaeta, J.J. Yoo, A. Atala, *Int. J. Impot. Res.* 19 (2007) 602–609.
 [14] N.P. Ziats, K.M. Miller, J.M. Anderson, *Biomaterials* 9 (1988) 5–13.
 [15] A.L. Brown, T.T. Brook-Allred, J.E. Waddell, J. White, J.A. Werkmeister, J.A. Ramshaw, D.J. Bagli, K.A. Woodhouse, *Biomaterials* 26 (2005) 529–543.
 [16] S.Y. Chun, G.J. Lim, T.G. Kwon, E.K. Kwak, B.W. Kim, A. Atala, J.J. Yoo, *Biomaterials* 28 (2007) 4251–4256.
 [17] R.A. Dawson, N.J. Goberdhan, E. Freedlander, S. MacNeil, *Burns* 22 (1996) 93–100.
 [18] W.P. Daley, S.B. Peters, M. Larsen, *J. Cell. Sci.* 121 (2008) 255–264.
 [19] D. Aharoni, I. Meiri, R. Atzmon, I. Vlodayvsky, A. Amsterdam, *Curr. Biol.* 7 (1997) 43–51.
 [20] J. Hodde, *Tissue Eng.* 8 (2002) 295–308.
 [21] R.A. Santucci, T.D. Barber, *Int. Braz. J. Urol.* 31 (2005) 192–203.
 [22] F. Mohamed, C.F. van der Walle, *J. Pharm. Sci.* 97 (2008) 71–87.

- [23] M. Talja, T. Valimaa, T. Tammela, A. Petas, P. Tormala, J. Endourol. 11 (1997) 391–397.
- [24] N. Ashammakhi, P. Rokkanen, *Biomaterials* 18 (1997) 3–9.
- [25] A.U. Daniels, M.K. Chang, K.P. Andriano, *J. Appl. Biomater.* 1 (1990) 57–78.
- [26] D.W. Hutmacher, J.T. Schantz, C.X. Lam, K.C. Tan, T.C. Lim, *J. Tissue Eng. Regen. Med.* 1 (2007) 245–260.
- [27] Z. Ma, Z. Mao, C. Gao, *Colloids Surf. B Biointerfaces* 60 (2007) 137–157.
- [28] R.A. Penkala, S.S. Kim, *Expert Rev. Med. Devices* 4 (2007) 65–72.
- [29] A. Atala, *Curr. Opin. Pediatr.* 18 (2006) 167–171.
- [30] R.E. De Filippo, J.J. Yoo, A. Atala, *Tissue Eng.* 9 (2003) 301–306.
- [31] G.E. Amiel, M. Komura, O. Shapira, J.J. Yoo, S. Yazdani, J. Berry, S. Kaushal, J. Bischoff, A. Atala, S. Soker, *Tissue Eng.* 12 (2006) 2355–2365.
- [32] S.J. Lee, J.J. Yoo, G.J. Lim, A. Atala, J. Stitzel, *J. Biomed. Mater. Res. A* 83 (2007) 999–1008.
- [33] L. Bacakova, E. Filova, F. Rypacek, V. Svorcik, V. Sary, *Physiol. Res.* 53 (Suppl. 1) (2004) S35–S45.
- [34] J.Y. Lai, P.Y. Chang, J.N. Lin, *J. Pediatr. Surg.* 40 (2005) 1869–1873.
- [35] S.J. Lee, G.J. Lim, J.W. Lee, A. Atala, J.J. Yoo, *Biomaterials* 27 (2006) 3466–3472.
- [36] D.O. Freytes, R.S. Tullius, J.E. Valentin, A.M. Stewart-Akers, S.F. Badylak, *J. Biomed. Mater. Res. A* (2008) doi:10.1002/jbm.a.31821. [Epub ahead of print].
- [37] B.G. Cilento, M.R. Freeman, F.X. Schneck, A.B. Retik, A. Atala, *J. Urol.* 152 (1994) 665–670.
- [38] A. Atala, J.P. Vacanti, C.A. Peters, J. Mandell, A.B. Retik, M.R. Freeman, *J. Urol.* 148 (1992) 658–662.
- [39] M.R. Freeman, J.J. Yoo, G. Raab, S. Soker, R.M. Adam, F.X. Schneck, F.X. Schneck, A.A. Renshaw, M. Klagsbrum, A. Atala, *J. Clin. Invest.* 99 (1997) 1028–1036.
- [40] M.C. Hiles, S.F. Badylak, L.A. Geddes, K. Kokini, R.J. Morff, *J. Biomed. Mater. Res.* 27 (1993) 139–144.